Geology

Hydrodynamic controls on alluvial ridge construction and avulsion likelihood in meandering river floodplains

--Manuscript Draft--

Manuscript Number:	G40104R1
Full Title:	Hydrodynamic controls on alluvial ridge construction and avulsion likelihood in meandering river floodplains
Short Title:	Hydrodynamic controls on alluvial ridge construction and avulsion likelihood
Article Type:	Article
Keywords:	Hydrodynamic; avulsion; floodplain; alluvial ridge
Corresponding Author:	Andrew Nicholas University of Exeter Exeter, Devon UNITED KINGDOM
Corresponding Author Secondary Information:	
Corresponding Author's Institution:	University of Exeter
Corresponding Author's Secondary Institution:	
First Author:	Andrew Nicholas
First Author Secondary Information:	
Order of Authors:	Andrew Nicholas
	Rolf Aalto
	Greg Sambrook Smith
	Arved Schwendel
Order of Authors Secondary Information:	
Manuscript Region of Origin:	
Abstract:	Existing models of alluvial stratigraphy often neglect the hydrodynamic controls on channel belt and floodplain sedimentation, and predict avulsion using topographic metrics, such as channel belt super-elevation. This study provides a first demonstration of the potential for simulating long-term river floodplain evolution (over >500 floods) using a process-based hydrodynamic model. Simulations consider alluvial ridge construction during the period leading up to an avulsion, and assess the controls on avulsion likelihood. Results illustrate that the balance between within-channel and overbank sedimentation exerts a key control on both super-elevation ratios and on the conveyance of water and sediment to the floodplain. Rapid overbank sedimentation creates high alluvial ridges with deep channels, leading to lower apparent super-elevation (the ratio of ridge height to channel depth), and implying reduced avulsion likelihood. However, channel deepening also drives a reduction in channel belt-floodplain connectivity, so that conveyance of water to the distal floodplain is concentrated in a declining number of channel breaches, which may favor avulsion. These results suggest that while super-elevation ratios in excess of a threshold value may be a necessary condition for a meandering river avulsion, avulsion likelihood may not be greatest where the super-elevation ratio is maximised. Instead, optimal conditions for avulsion may depend on channel-floodplain hydrodynamic connectivity, determined by the balance between coarse (channel bed forming) and fine (floodplain constructing) sediment delivery. These results highlight a need to rethink the representation of avulsion in existing models of alluvial architecture.

Publisher: GSA
Journal: GEOL: Geology
DOI:10.1130/G40104.1

Hydrodynamic controls on alluvial ridge construction and avulsion likelihood in meandering river floodplains

A.P. Nicholas[1], R.E. Aalto[1], G.H. Sambrook Smith[2], and A.C. Schwendel[3]

[1]Geography, College of Life and Environmental Sciences, University of Exeter, Exeter, EX4 4RJ, UK

[2]School of Geography, Earth and Environmental Sciences, University of Birmingham, Birmingham, B15 2TT, UK

[3]School of Humanities, Religion & Philosophy, York St John University, York, YO31 7EX, UK

ABSTRACT

Existing models of alluvial stratigraphy often neglect the hydrodynamic controls on channel belt and floodplain sedimentation, and predict avulsion using topographic metrics, such as channel belt super-elevation. This study provides a first demonstration of the potential for simulating long-term river floodplain evolution (over >500 floods) using a process-based hydrodynamic model. Simulations consider alluvial ridge construction during the period leading up to an avulsion, and assess the controls on avulsion likelihood. Results illustrate that the balance between within-channel and overbank sedimentation exerts a key control on both super-elevation ratios and on the conveyance of water and sediment to the floodplain. Rapid overbank sedimentation creates high alluvial ridges with deep channels, leading to lower apparent super-elevation (the ratio of ridge height to channel depth), and implying reduced avulsion likelihood. However, channel deepening also drives a reduction in channel belt-floodplain connectivity, so that

Publisher: GSA
Journal: GEOL: Geology
DOI:10.1130/G40104.1

conveyance of water to the distal floodplain is concentrated in a declining number of channel breaches, which may favor avulsion. These results suggest that while super-elevation ratios in excess of a threshold value may be a necessary condition for a meandering river avulsion, avulsion likelihood may not be greatest where the super-elevation ratio is maximised. Instead, optimal conditions for avulsion may depend on channel-floodplain hydrodynamic connectivity, determined by the balance between coarse (channel bed forming) and fine (floodplain constructing) sediment delivery. These results highlight a need to rethink the representation of avulsion in existing models of alluvial architecture.

INTRODUCTION

River avulsion involves the movement of alluvial channels, generally from areas of high topography (alluvial ridges) to low points in the fluvial landscape (e.g., distal flood basins). Such avulsions represent significant hazards with social and economic consequences (Sinha, 2009). They also exert a key control on the evolution of river and floodplain morphology (Slingerland and Smith, 2004) and the stratigraphic architecture of sedimentary basins (Hajek et al., 2010). Multiple factors are known to influence avulsion likelihood, including valley floor morphology, channel belt aggradation rate, flood magnitude, floodplain vegetation and the grain size characteristics of the river sediment load and valley deposits (Hajek and Wolinsky, 2012), yet avulsions remain difficult to predict. Process-based numerical models have provided important insights into aspects of avulsion mechanics, including the stability of bifurcation points in braided river networks (Bolla Pittaluga et al., 2003), delta channel branches (Edmonds and Slingerland, 2010) and crevasse splay sites where avulsions may occur (Slingerland and

Publisher: GSA
Journal: GEOL: Geology
DOI:10.1130/G40104.1

Smith, 1998). However, models of long-term fluvial landscape evolution and alluvial stratigraphy (Mackey and Bridge, 1995; Jerolmack and Paola, 2007; Karssenberg and Bridge, 2008) typically treat avulsion as a stochastic process, or predict avulsion using simple topographic metrics (e.g., the ratio of the down-valley to cross-valley surface gradients, or the channel belt super-elevation above the distal floodplain normalized by the channel depth). Such models tend to neglect or simplify the role of hydrodynamics, because solution of the governing equations describing fluid flow is computationally expensive. Herein, we seek to investigate the hydrodynamic controls on floodplain evolution and alluvial ridge construction in the period prior to an avulsion, and the implications for the prediction of avulsion likelihood.

METHODS

Floodplain evolution was simulated using a new numerical model of flow, overbank sedimentation and meander migration. The simulations reported here do not represent specific rivers, but provide insight into the general behavior of large meandering sand-bed rivers, and the construction of floodplain topography in the period between avulsions. Details of the modeling approach are provided in the Data Repository. In summary, the model solves the depth-averaged shallow-water equations and an advection-diffusion equation representing suspended sediment transport and overbank deposition for three grain sizes (sand, silt and clay). These equations are solved in the channel along a series of rectangular cross-sections (using a 1D numerical scheme) and on a grid of cells representing the floodplain (using a 2D scheme). A sequence of floods is simulated, each with the same hydrograph of 20 days duration, with peak and minimum discharges of 15,000 m^3s^{-1} and 2,500 m^3s^{-1}. After each flood, channel

Publisher: GSA
Journal: GEOL: Geology
DOI:10.1130/G40104.1

migration is simulated using the meander migration model of Howard and Knutson (1984), which includes neck cutoffs. Channel cross-section bed elevations are then incremented by a defined rate of bed aggradation (A) that is constant for all locations (see Data Repository). The channel is assumed herein to have a fixed width of 500m (equal to twice the floodplain grid cell size of 250 m). The channel has a constant slope that is set by the slope of the floodplain and the channel sinuosity (i.e., channel bed elevations are not determined by sediment transport calculations). Channel depth is determined by the difference between the channel bed elevation and the floodplain height in adjacent grid cells. Initial conditions for each simulation are a planar floodplain with a constant downstream gradient, and a straight channel with a constant depth. The total sediment concentration (S) at the model inlet is defined as a function of discharge (Q) using a sediment rating curve (Syvitski, et al., 2000): $S = C\,Q^{1.5}$, where C is constant during each simulation, such that each flood has a constant sediment load. A set of 31 simulations, each consisting of 580 floods, were carried out (see Data Repository) to investigate the effects on floodplain and alluvial ridge construction of changes in bed aggradation rate (A) and suspended sediment load (controlled by varying C, which is proportional to the load and depends in nature on the controls on basin erosion rates, such as relief and climate).

RESULTS

During all simulations, channel and floodplain evolution follows a similar sequence (Fig. 1). The straight initial channel begins to meander and bend amplitude increases until cutoff occurs. The channel belt widens and the number of abandoned channel elements increases progressively. Near-channel sedimentation creates levees that

Publisher: GSA
Journal: GEOL: Geology
DOI:10.1130/G40104.1

92 are breached by lateral erosion where bend migration is rapid (at bend apices). Levee
93 breaches promote formation of splay deposits and sediment transport away from river.
94 Low lying abandoned channels are also sites of preferential sedimentation, and provide
95 pathways for sediment conveyance to the distal floodplain.

96 Deposition within the channel belt drives construction of an alluvial ridge (Fig. 2).
97 Progressive growth of the ridge alters inundation patterns so that flow is increasingly
98 restricted to conveyance paths associated with levee breaches and with low-lying distal
99 flood basins (Fig. 1C). This tendency is also driven by an increase in channel depth
100 resulting from sedimentation near the channel, particularly when the rate of channel bed
101 aggradation is low. There is also a transition in sedimentation styles, from splay
102 dominated deposition in the early stages of simulations, to infilling of cutoff channels in
103 the later stages.

104 Overall, floodplain inundation declines over the course of simulations. However,
105 inundation extent fluctuates between flood events, and significant conveyance of water to
106 the floodplain continues to occur in the latter stages of most simulations (Fig. 1D).
107 Fluctuations in inundation are driven by autogenic mechanisms that control channel-
108 floodplain connectivity (e.g., bend migration, creation and infilling of levee breaches,
109 bend cutoff) rather than differences in flood magnitude, which does not vary. The
110 tendency for floodplain inundation to decline is weaker where channel bed aggradation
111 rates are high (Fig. 1E) and where floodplain sedimentation rates are low (due to low
112 suspended sediment loads, as in Fig. 1F), both of which lead to lower channel depths.

113 All simulations are characterized by an alluvial ridge with a profile that is
114 concave in section (Fig. 2). Ridge height is influenced by the channel bed aggradation

Publisher: GSA
Journal: GEOL: Geology
DOI:10.1130/G40104.1

rate and the suspended sediment load, which set the rate of overbank sedimentation. Where the balance between bed aggradation and overbank sedimentation promotes an increase in channel depth, and hence bankfull discharge capacity, ridge height is limited by a decline in water and sediment delivery to the floodplain. Ridge height is also lower for finer suspended sediment, for which deposition declines more slowly away from the river, and for rapid channel migration, which reworks the alluvial ridge.

Avulsion likelihood can be related to the channel belt super-elevation ratio (β), defined as the height of the alluvial ridge divided by the channel depth (Hajek and Wolinsky, 2012). Figure 3A shows the relationships between β, the rate of channel bed aggradation (*A*), and the river suspended sediment load (controlled by *C*). Higher rates of channel bed aggradation promote greater values of β, which is consistent with existing understanding (Hajek and Wolinsky, 2012). Higher suspended sediment loads increase overbank sedimentation, creating higher alluvial ridges and deeper channels, the net effect of which is to reduce the β. This implies that systems with higher alluvial ridges and greater rates of floodplain aggradation may be less susceptible to avulsion, due to increased channel depth and bankfull flow capacity, compared to systems in which the channel belt aggrades more slowly. Clearly, the balance between in-channel and overbank sedimentation exerts a key control on β.

Most simulations reported here use a suspended sediment load composed of 5% sand, 75% silt and 20% clay. For simulations with a finer load (comprising 5% sand, 20% silt and 75% clay), increased sediment conveyance away from the channel leads to lower channel super-elevation values . For only one such simulation is $\beta>1$, which is commonly treated as a plausible threshold for avulsion (Jerolmack and Paola, 2007; Hajek and

Publisher: GSA
Journal: GEOL: Geology
DOI:10.1130/G40104.1

Wolinsky, 2012). Simulations in which bank erodibility was adjusted to be either 50% (or 150%) of the default erodibility value, induced changes in rates of bank migration of similar magnitude. However, the resulting changes in β were small (a 15% increase in β for less erodible banks and a 6.5% reduction in β for weaker banks). This suggests that the role of river migration in controlling the creation of flow breach points may be more significant than its influence on channel super-elevation.

One limitation of theory that predicts avulsion likelihood based on topographic indices is that it does not account for the hydrodynamic controls on channel-floodplain connectivity. Herein, we calculate a simple metric of floodplain hydrodynamic connectivity (α) that is equal to the mean depth of water on the floodplain after the flood peak, divided by the fraction of the channel-floodplain interface that is inundated (the location of this interface is illustrated in Fig. 1E). Figure 3b shows that in general, for a given rate of channel bed aggradation, higher suspended sediment loads (controlled by *C*) promote greater inter-flood variability in α and higher peak values of α as the alluvial ridge develops. This inter-flood variability in α is a product of changes in channel-floodplain connectivity driven by the autogenic mechanisms outlined above. Moreover, this autogenic signal is stronger in systems with high suspended sediment loads that promote rapid overbank sedimentation, deep channels and more localized bank breaching. Figure 3c illustrates values of α_{95}, the 95th percentile of α values, calculated over the final 200 floods of each simulation. Peak values of α_{95} occur where the channel bed aggradation rate is lowest and the suspended sediment load is highest. Such conditions maximise channel depth and the delivery of water to the floodplain through localized bank breaches.

Publisher: GSA
Journal: GEOL: Geology
DOI:10.1130/G40104.1

DISCUSSION

Existing models of alluvial stratigraphy often use topographic indices to predict avulsion likelihood (Mackey and Bridge, 1995; Jerolmack and Paola, 2007; Karssenberg and Bridge, 2008). Our results suggest that changes in channel depth are a key control on water and sediment conveyance to the floodplain, hence metrics that do not incorporate depth (e.g., slope ratios) may be less useful than metrics that do (e.g., super-elevation ratios). Moreover, the usefulness of super-elevation ratios may depend upon how channel depths are determined. For example, many models of alluvial stratigraphy estimate channel depth using hydraulic geometry relations that are under-pinned by the concept of river equilibrium or have no mechanistic basis (c.f. Paola, 2000). The applicability of such relations in aggrading (i.e., non-equilibrium) channels is questionable. Channel depth is more usefully conceptualised as a product of the difference between the rates of river bed and floodplain aggradation, where the latter reflects the balance between floodplain lowering due to channel migration (Lauer and Parker, 2008) and the rate of overbank sedimentation. By adopting such an approach here, albeit with a simplified representation of channel bed aggradation, we have shown that systems characterized by high suspended sediment loads that build large alluvial ridges may be characterized by deep channels and a lower than expected super-elevation ratio. This suggests that approaches that rely on equilibrium channel theory, or which treat the channel belt as a single unit that aggrades at a uniform rate, rather than resolving channel and floodplain aggradation separately, may have limited utility for representing avulsion likelihood.

The existence of a positive correlation between channel super-elevation and avulsion likelihood is a principle that is firmly established in alluvial sedimentology

Publisher: GSA
Journal: GEOL: Geology
DOI:10.1130/G40104.1

(Hajek and Wolinsky, 2012). Our results show that growth of an alluvial ridge is associated with changes in water and sediment conveyance to the floodplain that are controlled by changes in channel depth, and by inter-flood variability in channel-floodplain connectivity driven by autogenic mechanisms. We hypothesize that avulsion likelihood will be maximised in systems where water conveyance to the floodplain is concentrated (e.g., in a small number of breach points), rather than where floodwater is transferred to the floodplain over a large fraction of the channel belt-floodplain interface, because concentrated flow will be associated with greater erosion potential. Our results suggest that the former condition is favored by high suspended sediment loads that build deep channels and infill some levee breaches so that conveyance to the floodplain is localized. However, these conditions do not yield the highest super-elevation ratios, hence interpretation of such metrics as simple indicators of avulsion likelihood is problematic.

We propose that, in low gradient meandering rivers such as those considered here, conditions for avulsion are optimised where the balance of bedload and suspended load favors two conditions: (1) sufficient channel bed aggradation to maintain water and sediment delivery to the floodplain and thus create an alluvial ridge; (2) sufficient suspended load to allow the construction of deep channels characterized by localized channel-floodplain connectivity, and focused flow conveyance along potential avulsion pathways. While super-elevation ratios in excess of a threshold value may be a necessary condition for a meandering river avulsion, it is not certain that avulsion likelihood will be greatest where the super-elevation ratio is maximised.

Publisher: GSA
Journal: GEOL: Geology
DOI:10.1130/G40104.1

Our results do not consider situations in which the rate of channel bed aggradation greatly exceeds the rate of overbank sedimentation, such that the channel is filled rapidly and avulsions are frequent. Moreover, our assumption of spatially and temporally uniform channel aggradation is more applicable in lowland rivers, and is not representative of environments characterized by episodic and/or localized channel aggradation (e.g., upland rivers and alluvial fans). Because our model simulations prescribe the channel bed aggradation rate and assume that the channel width is fixed, they likely under-estimate the potential for complex behavior resulting from changes in the ratio of coarse to fine sediment supply. Despite that, these results demonstrate the potential for investigating the controls on floodplain construction over periods of centuries to millennia, using a model underpinned by a physics-based treatment of hydrodynamics (i.e., the shallow water equations). These simulations highlight a need to rethink existing conceptual models of avulsion likelihood and their implications for the interpretation of the alluvial record. In the future, application of high resolution (channel-resolving) 2D morphodynamic models can afford further insight into the controls on avulsion (e.g., Hajek and Edmonds, 2014). More specifically, our results suggest that such models may be particularly important tools for understanding how changes in the ratio of coarse-to-fine sediment supply promote changes in channel morphology (e.g., cross-sectional form), local bed aggradation rates, and sediment exchanges with the floodplain.

SUMMARY

This study provides a first demonstration of the potential for simulating alluvial ridge construction and floodplain evolution using a process-based model under-pinned by

the shallow water equations. Simulations illustrate that hydrodynamic conditions that likely promote avulsion (e.g., water delivery to the floodplain through a restricted number of channel breach points) are not necessarily associated with conditions that maximize established proxies for avulsion likelihood (e.g., channel belt super-elevation normalized by channel depth). These results highlight a need to rethink the representation of avulsion in models of alluvial architecture and sedimentary basin filling. Specifically, we hypothesize that the ratio of coarse to fine sediment delivery to rivers exerts a key control on avulsion frequency that is not accounted for well by existing models. Moreover, our results suggest that improved representation of avulsion in models of alluvial architecture necessitates the decoupling of channel bed and channel belt aggradation rates, and further consideration of the morphodynamic conditions under which channel-floodplain hydrodynamic connectivity is primed to optimise avulsion likelihood.

ACKNOWLEDGMENTS

This work was funded by UK NERC grants NE/H009108/1 and NE/H007288/1. Simulations were performed using the University of Exeter Supercomputer. We thank Renato Almeida, Peter Burgess and Cari Johnson for their thoughtful reviews that helped us improve the manuscript.

REFERENCES CITED

Bolla Pittaluga, M., Repetto, R., and Tubino, M., 2003, Channel bifurcation in braided rivers: Equilibrium configurations and stability: Water Resources Research, v. 39, p. 1046, 10.1029/2001WR001112.

Edmonds, D.A., and Slingerland, R.L., 2010, Significant effect of sediment cohesion on delta morphology: Nature Geoscience, v. 3, p. 105–109, https://doi.org/10.1038/ngeo730.

Hajek, E.A., and Edmonds, D.A., 2014, Is river avulsion controlled by floodplain morphodynamics: Geology, v. 42, p. 199–202, https://doi.org/10.1130/G35045.1.

Hajek, E.A., and Wolinsky, M.A., 2012, Simplified process modelling of river avulsion and alluvial architecture: Connecting models and field data: Sedimentary Geology, v. 257–260, p. 1–30, https://doi.org/10.1016/j.sedgeo.2011.09.005.

Hajek, E.A., Heller, P.L., and Sheets, B.A., 2010, Significance of channel-belt clustering in alluvial basins: Geology, v. 38, p. 535–538, https://doi.org/10.1130/G30783.1.

Howard, A.D., and Knutson, T.R., 1984, Sufficient conditions for river meandering: A simulation approach: Water Resources Research, v. 20, p. 1659–1667, https://doi.org/10.1029/WR020i011p01659.

Jerolmack, D.J., and Paola, C., 2007, Complexity in a cellular model of river avulsion: Geomorphology, v. 91, p. 259–270, https://doi.org/10.1016/j.geomorph.2007.04.022.

Karssenberg, D., and Bridge, J.S., 2008, A three-dimensional numerical model of sediment transport, erosion and deposition within a network of channel belts, floodplain and hill slope: Extrinsic and intrinsic controls on floodplain dynamics and alluvial architecture: Sedimentology, v. 55, p. 1717–1745, https://doi.org/10.1111/j.1365-3091.2008.00965.x.

Lauer, J.W., and Parker, G., 2008, Modeling framework for sediment deposition, storage, and evacuation in the floodplain of a meandering river: Theory: Water Resources Research, v. 44, p. W04425, 10.1029/2006WR005528.

Mackey, S.D., and Bridge, J.S., 1995, Three-dimensional model of alluvial stratigraphy; theory and applications: Journal of Sedimentary Research, Section B: Stratigraphy and Global Studies, v. 65, p. 7–31, https://doi.org/10.1306/D42681D5-2B26-11D7-8648000102C1865D.

Paola, C., 2000, Quantitative models of sedimentary basin filling: Sedimentology, v. 47, p. 121–178, https://doi.org/10.1046/j.1365-3091.2000.00006.x.

Sinha, R., 2009, The Great avulsion of Kosi on 18 August 2008: Current Science, v. 97, p. 429–433.

Slingerland, R.L., and Smith, N.D., 1998, Necessary conditions for a meandering-river avulsion: Geology, v. 26, p. 435–438, https://doi.org/10.1130/0091-7613(1998)026<0435:NCFAMR>2.3.CO;2.

Slingerland, R.L., and Smith, N.D., 2004, River Avulsions and Their Deposits: Annual Review of Earth and Planetary Sciences, v. 32, p. 257–285, https://doi.org/10.1146/annurev.earth.32.101802.120201.

Syvitski, J.P., Morehead, M.D., Bahr, D.B., and Mulder, T., 2000, Estimating fluvial sediment transport: The rating parameters: Water Resources Research, v. 36, p. 2747-2760, https://doi.org/10.1029/2000WR900133.

FIGURE CAPTIONS

Figure 1. Spatial patterns of simulated deposit thickness for individual floods. Panels A to D show deposits for four floods in a simulation for which $C = 0.003$ and $A = 0$ m flood^{-1}. Panels E and F show deposits for two other simulations with contrasting values of C and

Publisher: GSA
Journal: GEOL: Geology
DOI:10.1130/G40104.1

296 *A*, but for the same flood shown in panel D. Flow is from left to right. Green indicates
297 areas with deposit thickness $<10^{-6}$ m. The main channel cells are shaded black. The
298 magenta dashed line in panel E denotes the channel-floodplain interface, used in the
299 calculation of the floodplain hydrodynamic connectivity metric (α).
300
301 Figure 2. Floodplain cross-sections at points located midway along the model domain.
302 Each panel shows results from a single simulation with different values of *A* and *C*.
303 Results are shown at four points in time, where *T* indicates the number of floods that have
304 been simulated.
305
306 Figure 3. A: Super-elevation ratio (β), which equals the height of the alluvial ridge
307 divided by the mean channel depth, plotted against the prescribed channel bed
308 aggradation rate (*A*). Each point represents the model results at the end of a single
309 simulation. The legend indicates the values of *C* used. (F) indicates a fine sediment load
310 with 5% sand, 20% silt and 75% clay. In all other simulations, the sediment load
311 comprises 5% sand, 75% silt and 20% clay. (L) indicates bank erodibility that is 50% of
312 the default value. (H) indicates bank erodibility that is 150% of the default value. Where
313 (L) or (H) is not specified, simulations use the default erodibility. B: Time series of the
314 parameter α, which is equal to the mean depth of floodwater on the floodplain 60% of the
315 way through the flood, divided by the fraction of the interface between the channel and
316 floodplain that is inundated (see dashed line in Fig 1E). Results are shown for three
317 simulations with contrasting values of *C* (*A* = 0.018 m flood^{-1} in all cases). C: 95th
318 percentile of the values of the parameter α calculated over the final 200 floods in each

Publisher: GSA
Journal: GEOL: Geology
DOI:10.1130/G40104.1

simulation, plotted against the prescribed channel bed aggradation rate (*A*). Symbols are the same as those used in Figure 3A.

1GSA Data Repository item 2018xxx, xxxxxxxx, is available online at http://www.geosociety.org/datarepository/2018/ or on request from editing@geosociety.org.

Figure 1

Click here to download Figure Figure 1_final.png

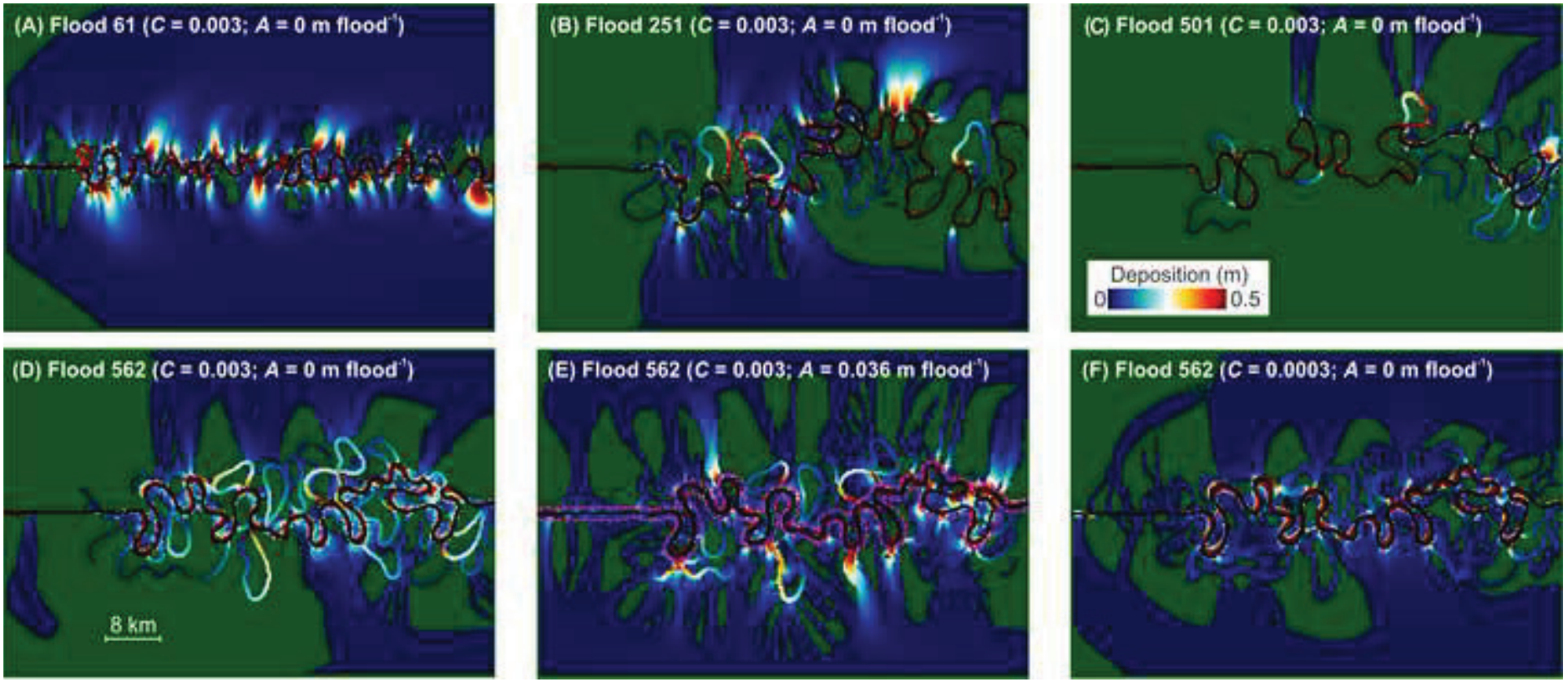

Figure 2

Click here to download Figure Figure 2_final.png

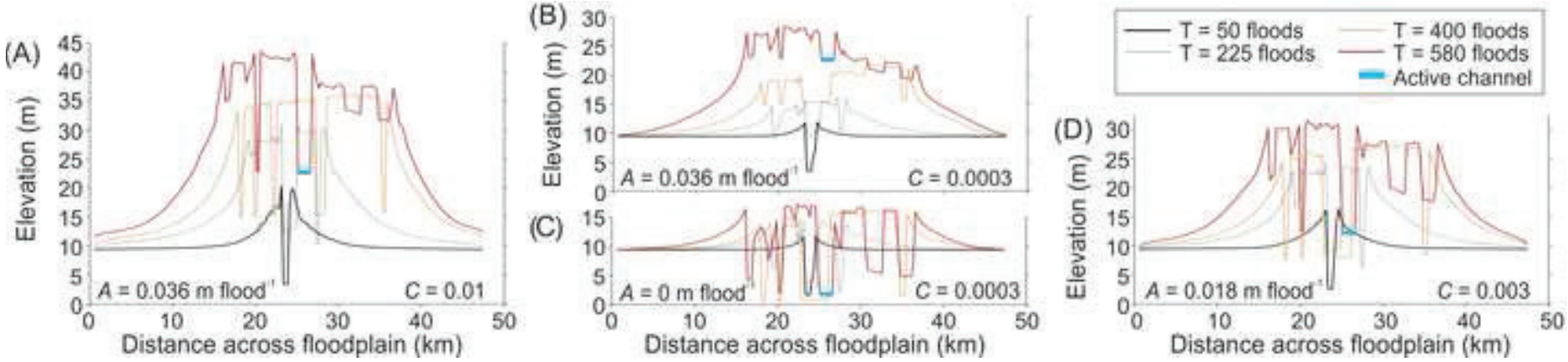

Figure 3

Click here to download Figure Figure 3_final.png